A spectral model for investigation of amplifying baroclinic waves

By LARS MOEN, *The Swedish Meteorological and Hydrological Institute*

(Manuscript received August 14, 1973; revised version January 2, 1974)

ABSTRACT

A spectral quasi-geostrophic model with vertical derivatives approximated by finite differences is used to study the effect of different vertical resolutions on the behaviour of baroclinic waves. The effect of the small terms in the complete vorticity and thermodynamic equations is also investigated. These terms are treated separately and modify a first order growing wave and the induced zonal field. The baroclinic instability with respect to first order perturbations is computed for different x- and y-wave numbers. Numerical experiments indicate that a low vertical resolution is most serious when the horizontal scale is small. High resolution models have a significantly higher instability in the short wave interval 1 000–2 000 km and the instability is split into two separate maxima. The secondary maximum at the shortest wavelengths is very sensitive to changes in the static stability and is also present in a linearized primitive model. A necessary spacing needed to resolve this instability is of the order of 5 vertical levels and 150 km horizontal gridlength. The effect of the vertical resolution on the induced zonal and second order field was found to be very small. The contribution from the small terms in the complete equations is mainly a deepening of the cyclones and a weakening of the anticyclones and an increased cyclonic circulation in the eastern parts of the upper troughs and ridges. The relative importance of each of the small terms is studied and it is concluded that it is important to keep them all.

1. Introduction

The development and structure of largescale eddies in a baroclinic zonal flow is a classical problem in meteorology and has been extensively investigated by many authors. By the method of small perturbations imposed on a steady barcolinic current the equations can be linearized and special solutions to the problem can be obtained. The works by Charney (1947), Eady (1949) and Kuo (1952, 1953) can be mentioned as examples.

Others have approached the problem by the use of numerical prediction models (cf., e.g. Phillips, 1956; Hinkelmann, 1959; Huss & Mintz, 1962). The equations are made algebraic by the introduction of finite differences in place of all derivatives.

The perturbation method is limited to small disturbances and all non-linear interactions are excluded. The numerical prediction models do not have these limitations, but systematic investigations with these models can be very cumbersome due the high number of dependent variables. An alternative method by which the number of variables can be considerably reduced is the use of some spectral model. The dependent variables are expanded into a series of orthogonal functions. The coefficients of these functions become the new dependent variables. By a truncation of the series, the number of variables and ordinary differential equations is made finite. The resulting system of equations, which can describe non-linear interactions, has often the advantage that it can be solved with relatively little effort. The spectral method was used for example by Bryan (1959) and Lorenz (1960*a*).

In the present investigation orthogonal functions are used in the horizontal, but finite differences in the vertical. The results tell us something both about the properties of the governing equations and about numerical prediction models. The purpose is to study the effect on a developing cyclone of two possible improvements of the quasi-geostrophic model, namely a larger vertical resolution and the use of the vorticity and the thermodynamic equations in their complete form.

The equations for the general model are derived in the sections 2, 3 and 4. For application to the specific problem, further simplifications are introduced in section 5 by truncation of the series of spectral functions and splitting of the solution into a first order solution and a second order response to this one, caused by the small terms. In section 6 it is shown that the first order flow can be described by a set of linear equations and can be solved as an algebraic eigenvalue problem. By non-linear interactions the zonal flow is modified and second order perturbations are created. These processes can be studied by use of time step integrations as described in section 7. The results of the numerical experiments are discussed in section 8.

List of notations not defined in he text:

- x, y distance eastward and northward respectively
- p pressure
- t time
- ψ streamfunction
- χ velocity potential
- ω dp/dt, vertical velocity in the p-system
- ϕ geopotential
- Θ potential temperature
- f, f_0 Coriolis parameter
- β df/dy

2. The basic equations

Many numerical prediction models for atmospheric flow are based on the following equations:

I. The vorticity equation:

$$\frac{\partial}{\partial t}(\nabla^2\psi) = -J(\psi, \nabla^2\psi + f) + f\frac{\partial\omega}{\partial p} + W'$$

where

$$W' = \nabla^2\psi\frac{\partial\omega}{\partial p} - \omega\frac{\partial}{\partial p}(\nabla^2\psi) - \nabla\omega\cdot\nabla\left(\frac{\partial\psi}{\partial p}\right)$$

$$-\nabla\chi\cdot\nabla(\nabla^2\psi + f)$$

II. The thermodynamic equation:

$$\frac{\partial}{\partial t}\left(\frac{\partial\psi}{\partial p}\right) = -J\left(\psi, \frac{\partial\psi}{\partial p}\right) - \frac{s}{f}\omega + W''$$

where

$$W'' = -\nabla\chi\cdot\nabla\left(\frac{\partial\psi}{\partial p}\right)$$

and

$$s = \frac{1}{\theta}\frac{\partial\phi}{\partial p}\frac{\partial\theta}{\partial p}$$

is a measure of the static stability which is assumed to be a function of pressure only.

III. The continuity equation:

$$\nabla^2\chi = -\frac{\partial\omega}{\partial p}$$

The terms denoted by W in the vorticity and thermodynamic equations are usually neglected. In this study we will, however, include W in the solution by treating it as a second order effect modifying the first order solution obtained with $W = 0$.

The four terms in W' describe the following physical effects:

I. relative vorticity—divergence effect,
II. vertical advection of relative vorticity,
III. twisting effect,
IV. advection of vorticity by the divergent wind.

The only term neglected in the vorticity equation is the divergent part of the s.c. twisting effect, $J(\omega, \partial\chi/\partial p)$. The magnitude of this term is one order smaller than all other terms in W' (see Pedersen, 1971).

W'' expresses temperature advection by the divergent wind.

It is assumed in the thermodynamic equation that the balance between the mass field and the non-divergent wind field is described by the geostrophic relation

$$\phi = f_0\psi$$

Due to this simplified form of the balance equation, the model does not exactly conserve the sum of kinetic energy and available potential energy (Lorenz, 1960*b*). The restriction on the static stability also limits the description of the static stabilization accompanying the release of kinetic energy.

As will be shown, the inclusion of the small terms in the vorticity and thermodynamic equations, although not energy consistent, adds features to the development of individual cyclones which are typical for the real atmosphere.

Friction and heating are already neglected and the Coriolis parameter f will be treated as a constant where it appears as a coefficient (β-plane approximation).

The system of equations can then be written as

$$\left\{\begin{aligned}
&\frac{\partial}{\partial t}(\nabla^2\psi) = -J(\psi, \nabla^2\psi) - \beta\frac{\partial\psi}{\partial x} + f_0\frac{\partial\omega}{\partial p} + W' \\
&\frac{\partial}{\partial t}\left(\frac{\partial\psi}{\partial p}\right) = -J\left(\psi, \frac{\partial\psi}{\partial p}\right) - \frac{s}{f_0}\omega + W'' \\
&\nabla^2\chi = -\frac{\partial\omega}{\partial p} \\
&W' = (\nabla^2\psi)\frac{\partial\omega}{\partial p} - \omega\frac{\partial}{\partial p}(\nabla^2\psi) - \nabla\omega\cdot\nabla\left(\frac{\partial\omega}{\partial p}\right) \\
&\qquad - \nabla\chi\cdot\nabla(\nabla^2\psi) - \beta\frac{\partial\chi}{\partial y} \\
&W'' = -\nabla\chi\cdot\nabla\left(\frac{\partial\psi}{\partial p}\right)
\end{aligned}\right. \tag{1}$$

3. Expansion in orthogonal functions

Following Lorenz (1963*b*) we will expand the variables in a series of orthogonal functions and then truncate the series to include only those which are necessary to describe at least the main characteristics of the phenomena to be studied.

We write

$$\psi(x, y, p, t) = \sum_i \psi_i(p, t)\, F_i(x, y)$$

$$\omega(x, y, p, t) = \sum_i \Omega_i(p, t)\, F_i(x, y)$$

$$\chi(x, y, p, t) = \sum_i \chi_i(p, t)\, F_i(x, y)$$

vhere F_i are orthogonal functions satisfying

$$\overline{F_i F_j} = \delta_{ij} = \begin{cases} 1 & \text{if} \quad i = j \\ 0 & \text{if} \quad i \neq j \end{cases}$$

$$\nabla^2 F_i = -a_i^2 F_i$$

Here a_i is a constant and a bar denotes an area integral.

If a boundary exists

$$\frac{\partial F_i}{\partial s} = 0$$

everywhere on the boundary, $\partial/\partial s$ denoting a tangential derivative.

This boundary condition implies that the wind component normal to the boundary is zero for the non-divergent part of the flow but that the divergent wind can have a component across the boundary. Hence the expansion cannot be applied to a flow inside physical walls, but rather to a flow with open boundaries on which arbitrary restrictions are placed (compare numerical weather prediction models on limited areas).

The divergent wind is in the present study only affecting second order terms and the first order solution is completely independent of a divergent flow across the boundaries. The quasi-geostrophic approximation also guarantees that this flow is only a small part of the total flow.

The Jacobian of two orthogonal functions can be expanded in a series

$$J(F_j, F_k) = \sum_i c_{ijk} F_i \quad \text{where } c_{ijk} = \overline{F_i J(F_j, F_k)}$$

Similar expansions can be used in other non-linear terms, i.e.

$$F_j F_k = \sum_i d_{ijk} F_i \quad \text{where } d_{ijk} = \overline{F_i F_j F_k}$$

and

$$\nabla F_j \cdot \nabla F_k = \sum_i e_{ijk} F_i \quad \text{where } e_{ijk} = \overline{F_i \nabla F_j \cdot \nabla F_k}$$

The x- and y-derivatives in the β-terms must also be expanded:

$$\frac{\partial F_j}{\partial x} = \sum_i a_{ij} F_i \quad \text{where } a_{ij} = \overline{F_i \frac{\partial F_j}{\partial x}}$$

and

$$\frac{\partial F_j}{\partial y} = \sum_i b_{ij} F_i \quad \text{where } b_{ij} = \overline{F_i \frac{\partial F_j}{\partial y}}$$

By introducing these expressions into the system (1) all horizontal derivatives can be eliminated. In the next section the vertical derivatives will be approximated by finite differences and the non-linear system can in this way be transformed into a system of ordinary differential equations for the time derivatives of $\psi_i(n)$ and $\Omega_i(n)$, where n is an index denoting a pressure level. To be able to solve this system we must first compute all interaction coefficients a_{ij}, b_{ij}, c_{ijk}, d_{ijk} and e_{ijk}. Although many of the coefficients are identically zero, a rather small number of horizontal orthogonal functions F_i results in a large number of interaction coefficients. However, by a suitable truncation of the series we can reduce the system considerably but still retain a set of equations describing the characteristic features of a developing cyclone.

We chose horizontal orthogonal functions, F_i, of the following form:

$$F_{q0} = \sqrt{2} \cos (qly)$$

$$F_{qr} = 2 \sin (qly) \cdot \cos (rkx)$$

$$F'_{qr} = 2 \sin (qly) \cdot \sin (rkx)$$

where q and r are positive integers and l and k are wave numbers in the y- and x-directions respectively, $l = 2\pi/L$ and $k = 2\pi/K$.

The boundaries in the x-direction are placed at a distance $L/2$ from each other. In the other direction cyclical boundary conditions are applied.

The horizontal averages are computed over the area $0 < y < L/2$, $0 < x < K$.

4. The spectral model

By introducing the expansions defined in the last section into the vorticity and thermodynamic equations the variation in time of each spectral component can be described by the following two equations:

$$\left\{\begin{aligned} \frac{\partial \psi_i}{\partial t} &= \sum_{j>k} \frac{c_{ijk}(a_j^2 - a_k^2)}{a_i^2} \psi_j \psi_k + \sum_l \frac{\beta a_{il}}{a_i^2} \psi_l \\ &\quad - \frac{f_0}{a_i^2} \frac{\partial \Omega_i}{\partial p} + W'_i \qquad (2\,\text{a}) \\ \Omega_i &= \frac{f_0}{s} \left[\sum_{j>k} c_{ijk} \left(\frac{\partial \psi_j}{\partial p} \psi_k - \frac{\partial \psi_k}{\partial p} \psi_j \right) \right. \\ &\quad \left. - \frac{\partial}{\partial p} \left(\frac{\partial \psi_i}{\partial t} \right) + W''_i \right] \qquad (2\,\text{b}) \end{aligned}\right.$$

where W'_i and W''_i stand for the following terms

$$W'_i = \sum_j \sum_k \left[d_{ijk} \frac{a_j^2}{a_i^2} \psi_j \frac{\partial \Omega_k}{\partial p} - d_{ijk} \frac{a_k^2}{a_i^2} \Omega_j \frac{\partial \psi_k}{\partial p} + e_{ijk} \frac{1}{a_i^2} \Omega_j \frac{\partial \psi_k}{\partial p} - e_{ijk} \frac{a_j^2}{a_i^2 a_k^2} \psi_j \frac{\partial \Omega_j}{\partial p} \right] + \sum_k \left[b_{ik} \frac{\beta}{a_i^2 a_k^2} \frac{\partial \Omega_k}{\partial p} \right]$$

$$W''_i = - \sum_j \sum_k \left[e_{ijk} \frac{1}{a_j^2} \frac{\partial \Omega_j}{\partial p} \frac{\partial \psi_k}{\partial p} \right]$$

In these expressions the velocity potential χ has been eliminated by the use of the continuity equation, which can be written in spectral form as

$$a_i^2 \chi_i = \frac{\partial \Omega_i}{\partial p}$$

The derivatives with respect to pressure can be approximated by finite differences between pressure levels. The vertical structure of the model is shown in Fig. 1. Between the earth surface, where the pressure is assumed to be 1 000 mb, and the top of the atmosphere ($p = 0$) a number of N ψ-levels are aribitrarily placed. The stability s and the vertical velocity Ω are defined on levels half-ways between two successive ψ-levels.

The commonly used upper boundary condition in similar models is $\omega = 0$ at $p = 0$. However, to be able to use centered differences in all terms a ψ-level is needed at $p = 0$. The upper boundary condition chosen in the present model is that ψ is constant at $p = 0$, which means that no horizontal motion is allowed at this level. Although there seems to be no obvious

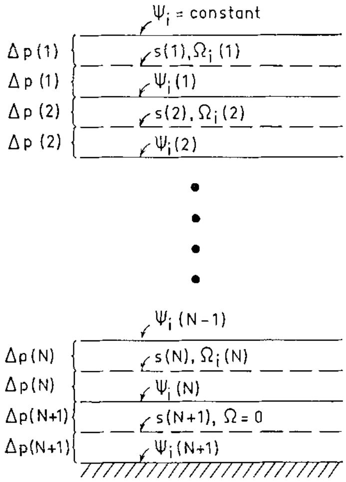

Fig. 1. Schematic representation of the vertical structure of the model.

physical justification for this condition, comparative computations (without the W-terms) with the two different upper boundary conditions showed no differences for short and medium-long waves, whereas only small differences in amplification rate and vertical structure of ultralong waves were obtained. As our main interest in the present investigation concerns the shorter part of the wavelength spectrum, the chosen boundary condition is satisfactory. For a study of the very long waves, penetrating through the stratosphere, a more thorough treatment of the upper boundary condition as well as a high vertical resolution in the upper atmosphere seems to be necessary.

The lower boundary condition is introduced by prescribing the variation of Ω at the lowest Ω-level. This level does not coincide with the earth surface which is the case in most other models. However, the present arrangement can be justified by noting that the constraint on Ω often is best valid at the top of the boundary layer. The choice of the lowest levels can thus be done so that the lowest Ω-level is placed at the mean position of the top of the boundary layer.

The vorticity equation in the form of equation (2a) is now applied at the ψ-levels 1, 2, ... N, and the thermodynamic equation (2b) at the Ω-levels 1, 2, ... N. The vertical derivatives are approximated by finite differences.

The vector $\mathbf{\Omega}_i$, consisting of the N elements $\Omega_i(1)$, $\Omega_i(2)$, ... $\Omega_i(N)$, can then be eliminated from the third term in the vorticity equation. The resulting equation expresses the time variation of the vector $\boldsymbol{\psi}_i$, consisting of the N elements $\psi_i(1)$, $\psi_i(2)$, ... $\psi_i(N)$.

In the second order terms W_i, the Ω-values are approximated by first order solutions of Ω_j and Ω_k. (The first order solutions are computed with $W_j = 0$ and $W_k = 0$ respectively. The numerical procedure is described in appendix *B*.)

After these manipulations the system of equations can be written in vector form in the following way.

$$\frac{d\boldsymbol{\psi}}{dt} = \sum_{j>k} \left[\frac{c_{ijk}(a_j^2 - a_k^2)}{a_i^2} (\mathbf{M}_1)_i \cdot \mathbf{X}_{jk} \right] + \sum_{l} \left[\frac{\beta a_{il}}{a_i^2} (\mathbf{M}_1)_i \cdot \boldsymbol{\psi}_l \right] - \sum_{j>k} \left[\frac{f_0^2 c_{ijk}}{a_i^2} (\mathbf{M}_2)_i \cdot \mathbf{Y}_{jk} \right] + \mathbf{W}_i' \tag{3a}$$

$$\mathbf{\Omega}_i = \sum_{j>k} [f_0 c_{ijk} \mathbf{M}_3 \cdot \mathbf{Y}_{jk}] + f_0 \mathbf{M}_4 \frac{d\boldsymbol{\psi}_i}{dt} + \mathbf{W}_i'' \tag{3b}$$

where

$$\mathbf{W}_i' = \sum_j \sum_k \left[\frac{d_{ijk}}{a_i^2} (\mathbf{M}_1)_i \cdot (\mathbf{P}_{jk} - \mathbf{Q}_{jk}) + \frac{e_{ijk}}{a_i^2} (\mathbf{M}_1)_i \cdot (\mathbf{R}_{jk} - \mathbf{S}_{jk}) \right] + \sum_k \left[\frac{\beta b_{ik}}{a_i^2} (\mathbf{M}_1)_i \cdot \mathbf{T}_k \right] + \sum_j \sum_k \left[\frac{f_0 e_{ijk}}{a_i^2} (\mathbf{M}_2)_i \cdot \mathbf{V}_{jk} \right]$$

$$\mathbf{W}_j'' = -\sum_j \sum_k [f_0 e_{ijk} \mathbf{M}_3 \cdot \mathbf{V}_{jk}]$$

$\boldsymbol{\psi}_i$, $\mathbf{X}_{jk}$, $\mathbf{Y}_{jk}$, $\mathbf{P}_{jk}$, $\mathbf{Q}_{jk}$, $\mathbf{R}_{jk}$, $\mathbf{S}_{jk}$, $\mathbf{T}_k$ and $\mathbf{V}_{jk}$ are all N-dimensional vectors with the following elements

$$\boldsymbol{\psi}_i = \{\psi_i(n)\}$$

$$\mathbf{X}_{jk} = \{\psi_j(n)\, \psi_k(n)\}$$

$$\mathbf{Y}_{jk} = \{\psi_j(n)\, \psi_k(n-1) - \psi_j(n-1)\, \psi_k(n)\}$$

$$\mathbf{P}_{jk} = \{\alpha(n)\, a_j^2\, \psi_j(n)\, (\Omega_k(n+1) - \Omega_k(n))\}$$

$$\mathbf{Q}_{jk} = \left\{ \frac{\alpha(n)}{4} a_k(\psi_k(n+1) - \psi_k(n-1))\,(\Omega_j(n+1) + \Omega_j(n)) \right\}$$

$$\mathbf{R}_{jk} = \left\{ \frac{\alpha(n)}{4} (\Omega_j(n+1) + \Omega_j(n))\,(\psi_k(n+1) - \psi_k(n-1)) \right\}$$

$$\mathbf{S}_{jk} = \left\{ \alpha(n) \frac{a_k^2}{a_j^2} (\Omega_j(n+1) - \Omega_j(n))\,\psi_k(n) \right\}$$

$$\mathbf{T}_k = \left\{ \frac{\alpha(n)}{a_k^2} (\Omega_k(n+1) - \Omega_k(n)) \right\}$$

$$\mathbf{V}_{jk} = \left\{ \frac{\alpha(n)\,\alpha(n-1)}{a_j^2(\alpha(n) + \alpha(n-1))} (\Omega_j(n+1) - \Omega_j(n-1)) \times (\psi_k(n) - \psi_k(n-1)) \right\}$$

where

$$\alpha(n) = \frac{1}{\Delta p(n) + \Delta p(n+1)}$$

$(\mathbf{M}_1)_i$, $(\mathbf{M}_2)_i$, $\mathbf{M}_3$, $\mathbf{M}_4$ and $\mathbf{M}_5$ are all $N \times N$-dimensional matrices:

$$\mathbf{M}_3 = \begin{bmatrix} \beta(1) & 0 & \dots & 0 \\ 0 & \beta(2) & \dots & 0 \\ \cdot & \cdot & \dots & \cdot \\ 0 & 0 & \dots & \beta(N) \end{bmatrix};$$

$$\mathbf{M}_4 = \begin{bmatrix} -\beta(1) & 0 & \dots & 0 & 0 \\ \beta(2) & -\beta(2) & \dots & 0 & 0 \\ \cdot & \cdot & \dots & \cdot & \cdot \\ 0 & 0 & \dots & \beta(N) & -\beta(N) \end{bmatrix};$$

$$\mathbf{M}_5 = \begin{bmatrix} -\alpha(1) & \alpha(1) & 0 & \dots & 0 \\ 0 & -\alpha(2) & \beta(2) & \dots & 0 \\ \cdot & \cdot & \cdot & \dots & \cdot \\ 0 & 0 & 0 & \dots & \alpha(N-1) \\ 0 & 0 & 0 & \dots & -\alpha(N) \end{bmatrix};$$

$$(\mathbf{M}_1)_i = \left(\mathbf{I} + \frac{f_0^2}{a_i^2} \mathbf{M}_5 \cdot \mathbf{M}_4 \right)^{-1}; \quad (\mathbf{M}_2)_i = (\mathbf{M}_1)_i \cdot \mathbf{M}_5 \cdot \mathbf{M}_3;$$

where

$$\beta(n) = \frac{1}{2s(n) \cdot \Delta p(n)}$$

$\mathbf{I}$ is the unit matrix.

Due to the boundary condition $\Omega(N+1)$, the streamfunction at the surface of the earth can be computed from the simple relation:

$$\frac{d\psi_i(N+1)}{dt} = \frac{d\psi_i(N)}{dt} + \sum_{j>k} [c_{ijk}\, Y_{jk}(N+1)] - \sum_j \sum_k [e_{ijk}\, V_{jk}(N+1)] \tag{4}$$

In the last term a non-centered difference has to be used.

By expansion of the dependent variables in a suitable series of orthogonal functions the partial differential system of equations (1) has been transformed to a system of ordinary differential equations, (3) and (4), with the coefficients of the orthogonal functions as new dependent variables. Each equation expresses the time derivative of one of the variables as a function of linear combinations of the variables or of products between the variables. Such equations can easily be integrated numerically or in some cases solved analytically.

The derived spectral model is quite generally formulated. The vertical spacing can be chosen arbitrarily as well as the vertical distribution of the static stability. The model can be extended by the introduction of physical effects such as friction and non-adiabatic heating.

By chosing a limited number of orthogonal functions, suitable to represent the problem of interest, the mathematical labour can be much reduced. Lorenz (1963*b*) applied the method to a two-layer model in his study of the mechanics of vacillation. Bengtsson (pers. com.) used a multi-level spectral model for the study of the behaviour of amplifying waves with respect to different vertical resolutions.

5. Truncation of the series expansion

In this study the spectral model will be used to investigate how a single baroclinic unstable wave is affected by different vertical resolutions and by the second order terms in the vorticity equation. We will therefore truncate the series of orthogonal functions to inlude only those functions, which are necessary in such a case. The problem of how the static stability and vertical wind shear affect the developing cyclone will not be treated here. A normal distribution of these parameters is used.

We first restrict the wave number spectrum to $q \leqslant 3$ and $r \leqslant 3$. The truncated series then contains 21 orthogonal functions.

The number of (i, j)-combinations in the interaction coefficients is then 441, and the number of triple combinations (i, j, k) is 9 261, but the computational work will be considerably reduced if the following relations are used

$$c_{i,j,k} = c_{k,i,j} = -c_{j,i,k}$$

$$d_{i,j,k} = d_{k,i,j} = d_{j,i,k}$$

$$e_{i,j,k} = e_{i,k,j}$$

A great number of the coefficients turns out to be identically equal to zero.

By studying the 21 functions and the interaction coefficients we will now pick out a set of suitable functions.

We first let the mean zonal westerly flow be represented by the function

$$F_1 = \sqrt{2} \cos ly$$

The corresponding zonal wind is zero at the boundaries of the channel and maximum in the middle of the channel.

Due to a vertical shear, this flow can be baroclinically unstable in which case perturbations will start to grow. We chose to study the perturbation represented by the following two functions

$$\begin{cases} F_A = 2 \sin ly \cdot \cos kx \\ F_B = 2 \sin ly \cdot \sin kx \end{cases}$$

The development of the perturbation F_A, F_B will be called the *first order solution.*

The effects on a zonal current due to the presence of simple unstable baroclinic waves have been analyzed by Phillips (1954).

The growing wave will, by non-linear interactions, set up a characteristic vertical circulation of Ferrel type. This induced circulation will modify the total zonal flow.

By studying the interaction coefficients c_{ijk} we find that the only non-zero interaction of this type is created by the function

$$F_3 = \sqrt{2} \cos 3ly$$

The motion connected with F_3 will be called *induced zonal flow.* First order perturbations and their interactions with the zonal flow have successfully been studied by use of simplified forms of the vorticity equation. The flow connected with F_1, F_A, F_B and F_3 will therefore be computed without the W-terms.

Restricting the energy to stay in the waves represented by the spectral functions F_1, F_A, F_B and F_3, one may ask to what degree these functions can reproduce motions in the real atmosphere. We first recall that the present model neglects friction and non-adiabatic heating, thus there is no mechanism for creation of zonal available potential energy, $\bar{A}$, by heating to the south and cooling to the north, no dissipation of eddy available energy, A', and no destruction of zonal and eddy kinetic energy, $\bar{K}$ and K', by friction. The total initial energy will be maintained in the system.

What will happen if we start with nearly all energy in the zonal flow and a weak perturbation? If the flow is baroclinically unstable K' is released by transformation from A'. At the same time the growing disturbance converts $\bar{A}$ into A'. Due to the eddy heat flux, an indirect circulation of Ferrel-type with sinking motion to the south and rising motion to the north starts to develop. This circulation increases $\bar{A}$ at the expense of $\bar{K}$ because of a negative correlation between temperature and vertical velocity. Thus an energy flow $\bar{K} \to \bar{A} \to A' \to K'$ will take place. A conversion from K' to $\bar{K}$ is impossible due to the simple geometry of the perturbation. Such a conversion takes place only if the u- and v-components of the perturbation wind are correlated.

Wiin-Nielsen (1962) has shown that the vertical wind shear decreases if the thermal waves on the average are lagging behind the waves in the mean flow. Since this arrangement is typical for a developing wave this means that the barolinic instability, which depends on the vertical wind shear, decreases and at last disappears. After this stage the energy conversions will take the opposite direction $K' \to A' \to \bar{A} \to \bar{K}$. The processes described will be repeated and a periodic oscillation in energy transfers will take place.

In the real atmosphere, however, $\bar{K}$ undergoes very small changes (see for ex. Wiin-Nielsen, 1964). Palmén & Newton (1969) point out the importance of the subtropic Hadley-circulation for the maintenance of the zonal flow. Computations of the rates of transfer of kinetic energy to the zonal current from the eddies, performed by Saltzman & Teweles (1964), show positive contributions from all wave numbers with maxima at wave numbers 2 and 7. The absence of these two processes, acting to maintain the zonal flow, may be responsible for the described energy oscillations in the present truncated spectral model.

The conclusion of this analysis is that we must restrict the investigation to the amplifying stage of the development. Due to the inability of the present low order spectral model to maintain the zonal flow energy, it is also logic to force the kinetic energy of the zonal wind to be constant in time by letting

$$\frac{d\psi_1(n)}{dt} = 0$$

At this point we introduce the W-terms in the equations and investigate the second order response to the first order and induced zonal field.

The strategy will be to use only those orthogonal functions which interact with F_1, F_A, F_B and F_3 through non-vanishing coefficients b_{ij}, d_{ijk} or e_{ijk}.

It turns out that the only functions with these properties are the following

$$\begin{cases} F_a = 2\sin ly \cdot \cos 2kx \\ F_b = 2\sin ly \cdot \sin 2kx \end{cases}$$

$$\begin{cases} F_c = 2\sin 2ly \cdot \cos kx \\ F_d = 2\sin 2ly \cdot \sin kx \end{cases}$$

$$\begin{cases} F_e = 2\sin 3ly \cdot \cos 2kx \\ F_f = 2\sin 3ly \cdot \sin 2kx \end{cases}$$

$$F_2 = \sqrt{2}\cos 2ly$$

We call the corresponding fields the *second order solution.*

The six functions $F_a - F_f$ represent three perturbations while F_2 represents a zonal field. These functions have no interaction with the first order and induced zonal fields through the advection terms, i.e. $c_{ijk} = 0$.

We have thus been able to reduce the number of spectral components, to simplify the system of equations and to split the solution into a first order solution and a second order response to this caused by second order terms added to the vorticity and thermodynamic equations.

6. First order solution

The first order solution is described by the three functions F_1, F_A and F_B. We have already assumed that the zonal flow is stationary. Equation (3a) applied on $\psi_A(n)$ and $\psi_B(n)$ then transforms to a system of linear equations with constant coefficients.

By introducing

$$U(n) = \sqrt{2}\, l\psi_1(n)$$

which is the maximum zonal wind on a pressure surface and using

$$c_{BA1} = -c_{AB1} = \frac{8\sqrt{2}\,kl}{3\pi}$$

the resulting system can be written as

$$\begin{cases} \dfrac{d}{dt}\boldsymbol{\psi}_A = -\mathbf{M}\cdot\boldsymbol{\psi}_B \\ \dfrac{d}{dt}\boldsymbol{\psi}_B = \mathbf{M}\cdot\boldsymbol{\psi}_A \end{cases} \tag{5}$$

where $\mathbf{M}$ is the $N \times N$ matrix

$$\mathbf{M} = \frac{k^3}{k^2+l^2}\mathbf{M}_1 \cdot \left[\mathbf{D}_U - \frac{\beta}{k^2}\mathbf{I} - \frac{f_0^2}{k^2}\mathbf{M}_5 \cdot \mathbf{M}_3 \cdot \mathbf{M}_U\right]$$

where

$$\mathbf{D}_U = \frac{8}{3\pi}\begin{bmatrix} U(1) & 0 & \dots & 0 \\ 0 & U(2) & \dots & 0 \\ \cdot & \cdot & \dots & \cdot \\ 0 & 0 & \dots & U(N) \end{bmatrix}$$

$$\mathbf{M}_U = \frac{8}{3\pi}\begin{bmatrix} 0 & 0 & \dots & 0 & 0 \\ -U(2) & U(1) & \dots & 0 & 0 \\ \cdot & \cdot & \dots & \cdot & \cdot \\ 0 & 0 & \dots & -U(N) & U(N-1) \end{bmatrix}$$

$$\mathbf{M}_1 = (\mathbf{M}_1)_A = (\mathbf{M}_1)_B$$

By introducing the complex vector

$$\mathbf{\Phi} = \boldsymbol{\psi}_A + i\boldsymbol{\psi}_B$$

the system (5) takes the form

$$\frac{d}{dt}\mathbf{\Phi} = i\mathbf{M}\cdot\mathbf{\Phi} \qquad (6)$$

Assuming a harmonic solution in time, i.e.

$$\mathbf{\Phi} = \bar{\mathbf{\Phi}}\, e^{i\nu t}$$

we can write (6) as

$$(\mathbf{M} - \nu\mathbf{I})\cdot\bar{\mathbf{\Phi}} = \mathbf{0} \qquad (7)$$

$\mathbf{I}$ is the unit matrix and $\mathbf{0}$ the null matrix. A non-trivial solution to (7)[1] requires the determinant of the matrix inside the parenthesis to vanish, which implies that ν are the eigenvalues of the matrix $\mathbf{M}$. Generally the solution results in complex frequencies $\nu = \nu_r + i\nu_i$ with the corresponding complex eigenvectors

$$\bar{\mathbf{\Phi}} = \bar{\mathbf{\Phi}}_r + i\bar{\mathbf{\Phi}}_i$$

The eigensolution of $\psi_A(n)$ and $\psi_B(n)$ can be written as

$$\begin{cases} \psi_A(n) = A\cdot e^{-\nu_i t}\sqrt{\bar{\phi}_r^2(n) + \bar{\phi}_i^2(n)}\cos(\nu_r t + \delta(n)) \\ \psi_B(n) = B\cdot e^{-\nu_i t}\sqrt{\bar{\phi}_r^2(n) + \bar{\phi}_i^2(n)}\sin(\nu_r t + \delta(n)) \end{cases}$$

[1] It may be noted that for $l = 0$ the equation (7) is similar to the baroclinic instability problem of perturbations on a zonal current, $\bar{U}(n)$, without variation in y-direction, if

$$\bar{U}(n) = \frac{8}{3\pi}U(n)$$

The factor $8/3\pi$ arises from the integrals $\overline{F_i F_i}$ and $c_{ijk} = \overline{F_i J(F_i, F_k)}$, the latter divided by the former:

$$\frac{\int_0^{\pi/l}\sin^3 ly\,dy}{\int_0^{\pi/l}\sin^2 ly\,dy} = \frac{8}{3\pi}$$

where $\delta(n)$ is the phase angle

$$\delta(n) = \operatorname{arctn}\left(\frac{\bar{\phi}_i(n)}{\bar{\phi}_r(n)}\right)$$

and A, B are arbitrary constants.

The eigenvalue problem (7) is solved by a numerical method for a specified vertical distribution of stability and zonal wind.

In the numerical treatment the matrix $\mathbf{M}$ is first scaled and normalized, then reduced to an upper-Hessenberg form by means of similarity transformations (Householder's method). After that the QR double-step iterative process is performed for extraction of eigenvalues and by use of inverse iteration the eigenvectors are computed.

7. The induced zonal flow and second order solution

The induced zonal flow, represented by the orthogonal function

$$F_3 = \sqrt{2}\cos 3\,ly$$

is created by a non-linear interaction with the first order perturbation. At the same time the induced zonal field will modify the perturbation.

The interaction coefficient has the value

$$C_{3BA} = -\frac{8\sqrt{2}}{5\pi}kl$$

The system of equations to be solved can easily be derived from the equations (3a) and (3b) ($W_i' = W_i'' = 0$). The time derivatives are replaced by finite differences and a numerical integration in time is performed. The initial state consists of a baroclinically unstable ψ_1-field and superimposed a very small perturbation in the $(\psi_A + \psi_B)$-field.

The equations for the second order fields are also derived from the system (3), but now with W_i included. The W_i-terms are evaluated from the vertical velocity and streamfunction fields obtained from the first order and induced zonal solutions. The numerical procedure can be found in appendix B.

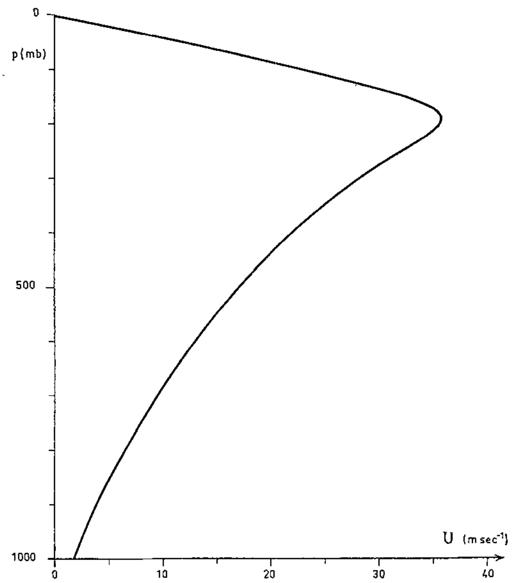

Fig. 2. Vertical wind profile $U(n) = 2l\psi_1(n)$.

8. Results

In the numerical experiments a zonal wind profile and a vertical variation of stability were used as shown in Figs. 2 and 3 (thick line).

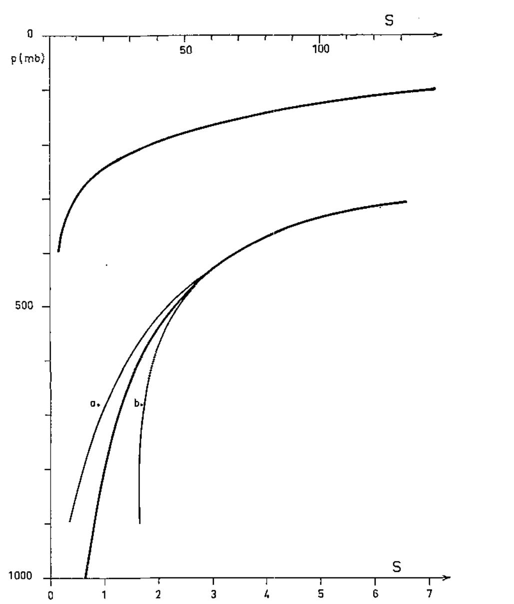

Fig. 3. Vertical distribution of static stability s (MTS-units).

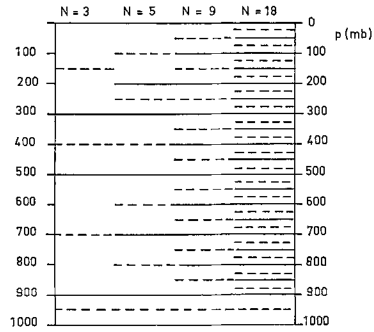

Fig. 4. The arrangement of levels in the four models used with different vertical resolution. The full lines indicate steamfunction levels and the dashed lines are levels for the vertical velocity.

These curves represent a rather typical baroclinically unstable middle-latitude mean flow.

Four different vertical resolutions were used corresponding to $N = 3$, 5, 9 and 18 (see Fig. 4). The streamfunction levels coincide with standard pressure levels. The Nth level is always placed at 900 mb so that the lower boundary condition for ω is valid at the same level in all versions.

In all experiments $f_0 = 1.03 \times 10^{-4}$ sec^{-1} and $\beta = 1.62 \times 10^{-11}$ m^{-1} sec^{-1}.

8.1. *First order solution*

The solution of the eigenvalue problem (7) results in a spectrum of N eigenvalues of ν. Most of these eigenvalues are real and correspond to neutral waves. The number of neutral waves increases as N increases. For almost all wavelengths there also exists a pair of complex frequencies representing one amplifying and one decaying wave.

The phase speeds of the stable and unstable waves as a function of wavelength in the x-direction are shown in Fig. 5 for a model with the vertical resolution $N = 9$. The behaviour of the waves is quite similar to what was found by Hirota (1968) for a model with no y-dependence and no vertical variation of the wind shear and static stability.

In Fig. 5 we recognize the neutral Rossby wave with a phase velocity strongly dependent on the wavelength, six neutral waves with nearly constant phase velocities and the phase velocity of one damped and one amplifying wave indicated by a dashed line. Using Hirota's terminology we identify two different modes of instability, the first mode with wavelengths less than approximately 6 000 km and the second mode for longer wavelengths.

Concerning the vertical structure of the unstable wave the result are in agreement with numerical experiments performed by Bengtsson (pers. comm.) with a similar model ($W = 0$). By the use of numerical integration in time he studied the evolution of the perturbation amplitude as depending upon the vertical resolution in the model. The wavelengths fell within the first mode of instability. The conclusion which can be drawn from his results and, as will be shown later, from the present investigation is that at least 5 vertical levels must be used if a good vertical representation of the first mode of unstable waves is desired.

We will now examine the unstable waves especially with respect to the influence of different vertical resolutions and wavelengths in the y-direction. Figs. 6–9 illustrate the amplification factor ν_i as a function of wavelength for $L = 2$ 500, 5 000, 10 000 and 15 000 km respectively. (The width of the zonal westerlies

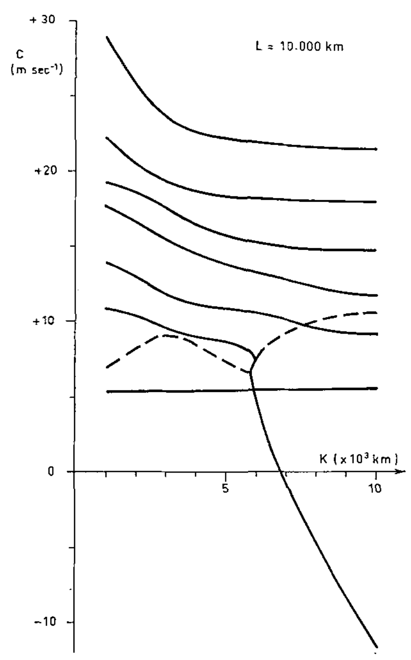

Fig. 5. Phase velocity as a function of wavelength K in the case of $N = 9$ and $L = 10$ 000 km. Full lines indicate neutral waves while the dashed line corresponds to the unstable waves.

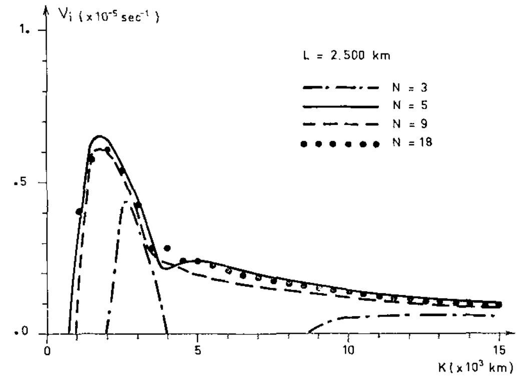

Fig. 6. Growth rates of unstable waves as a function of wavelength K and vertical resolution N. $L =$ 2 500 km.

is $L/2$.) It is seen that the maximum instability is achieved for the first mode of unstable waves whereas the second mode has significantly lower amplification. The transition from one mode to the other takes place at a shorter wavelength in the case of a narrow zonal jet, than for a broad zonal wind. For $L = 2$ 500 km the transition wavelength, which corresponds to the wavelength of the first "critical curve" in Hirota's article, is about 4 000 km, but for $L = 15$ 000 km approximately 6 000 km.

It can be noted that the growth rate is never zero (except for low vertical resolution) at the critical wavelengths as is the case in Hirota's model. This is best illustrated in the case of a narrow zonal flow.

In all computations a short wavelength limit to instability was found. As was shown by Green (1960) this cut-off does not occur in a

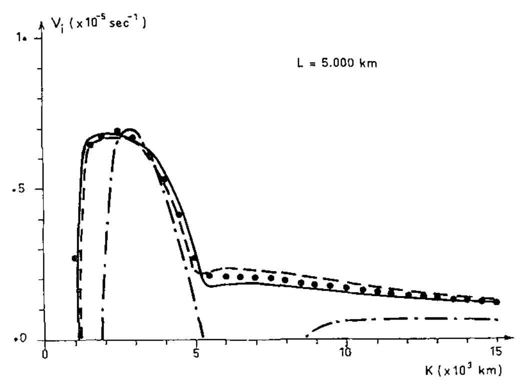

Fig. 7. Same as Fig. 6 but for $L = 5$ 000 km.

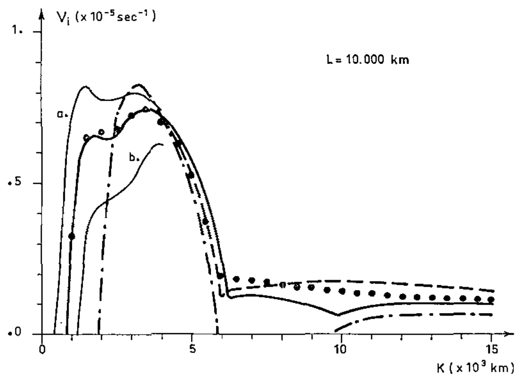

Fig. 8. Same as Fig. 6 but for $L = 10\,000$ km. The curves marked *a* and *b* correspond to different static stability as shown in Fig. 3.

vertical continuous β-plane model. The problem has been discussed by Bretherton (1966) who connected the existence of short unstable waves with the concept of "critical layer instability". This type of instability has a low growth rate and is limited vertically to a layer around a level where the real phase speed of the wave equals the zonal wind speed. Bretherton stated that critical layer instability is automatically eliminated from a problem if a continuously varying basic velocity is modelled by a finite number of layers. On the other hand Hirota reports no short wavelength cut-off for a 20-layer model. Brown (1969) illustrates by numerical experiments the widening of the band of unstable wavelengths when the vertical resolution is increased (table 4 in his appendix B), but unfortunately it is not clear if a cut-off exists for the highest resolution model. It is not the intention to solve the problem of critical layer instability and the short wavelength cut-off in the present investigation. Furthermore, considering the low growth rate connected with this instability, the meteorological significance is apperently rather small.

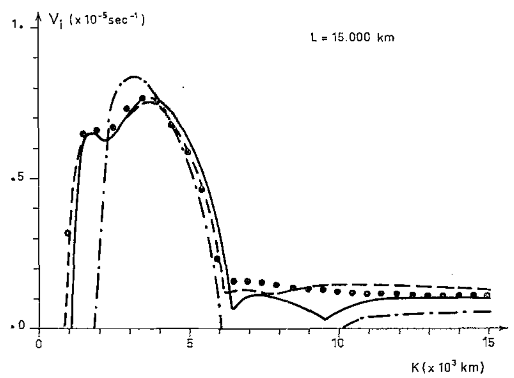

Fig. 9. Same as Fig. 6 but for $L = 15\,000$ km.

There is a remarkable difference between the growth rates for the low resolution model with $N = 3$ and for the higher resolutions. The difference between computations with $N = 5$, 9 and 18 is very small, especially for the first mode of unstable waves. $N = 5$ shows, however, a somewhat weaker instability in the second mode when the zonal wind is broad ($L = 10\,000$ km and 15 000 km).

The effect of a low resolution is most serious when the scale is small in the y-direction, both with regard to the wavelength of maximum instability and the numerical value of the maximum growth rate. The amplification of the second mode of unstable waves is completely absent in the wavelength interval 4 000–9 000 km when $N = 3$.

Two striking characteristics of the high resolution models as compared to the 3-level model are the significantly higher instability for very short waves in the interval 1 000–2 000 km and the splitting of the first mode instability into two separate maxima as L increases.

By the use of these results we have a possibility to get an idea about what degree of resolution both in the vertical and in the horizontal direction is meaningful and the relation between the two scales. For example, it is obvious that if we use a vertical resolution of $N = 3$ it is meaningless to have a gridlength shorter than about 250 km. (We assume that 8 gridlengths are necessary to describe a horizontal wave.)

Fig. 10 shows the eigenvector amplitude $(\bar{\phi}_r^2 + \bar{\phi}_i^2)^{1/2}$ and the corresponding phase angle δ for the unstable wave as a function of pressure. The vertical resolution in $N = 9$ and the wavelength in the y-direction is $L = 10\,000$ km. The maximum value of the amplitude is arbitrarily chosen to 1.0 and the phase angle is set zero at the level $n = N$.

The second mode of unstable waves, represented by $K = 8\,000$ km in the figure, shows a typical vertical structure with one amplitude maximum at higher levels and one maximum at the bottom of the atmosphere. The total phase difference is approximately π radians which means that a low pressure maximum in

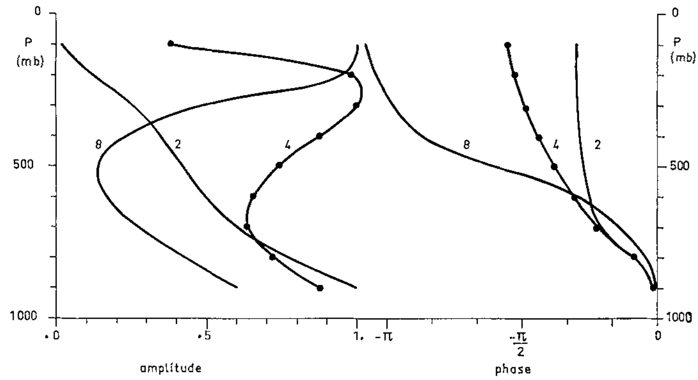

Fig. 10. Vertical structure of the unstable mode for the wavelengths $K = 2\ 000$ km, $K = 4\ 000$ km, and $K = 8\ 000$ km (denoted by 2, 4, and 8, respectively). $N = 9$ and $L = 10\ 000$ km. The dots are the results of a 7-day numerical integration with $K = 4\ 000$ km. The maximum amplitudes are arbitrarily set equal to 1 and the phase angle at the level N equal to 0.

the lower atmosphere corresponds to a high pressure maximum at higher levels and vice versa.

The curves for $K = 4\ 000$ km and $K = 2\ 000$ km fall within the region of the first mode of instability, the former near the main maximum of instability and the latter near the secondary maximum.

The longer wave has also one amplitude extreme in the upper atmosphere, at 200–300 mb, and another maximum at the lowest level. The total backward tilting of the disturbance is about $\pi/2$. The shorter wave has quite different characteristics. This disturbance is concentrated to the lower atmosphere with a nearly linear upward decrease of the amplitude. The total tilting of the wave is only $\pi/4$. The phase angle is nearly constant for levels above 600 mb. Similar results are reported by Simons (1972).

The secondary instability maximum at short wavelengths is very sensitive to changes in the static stability in the lower part of the atmosphere. This is demonstrated in Fig. 8 in which the thin curves, marked a and b, show the amplification for $N = 9$ in the case of low and high static stability respectively. The corresponding stabilities can be found in Fig. 3.

Brown (1969) obtained a double maximum of instability for a model that included both barotropic and baroclinic instability, probably as a result of the combined effects of these two different kinds of instability. In the present experiment, however, there is no barotropic instability present.

Although not discussed in the text, Simons' (1972) results from a purely baroclinic model indicate a secondary maximum of instability for short wavelengths in the case of a high vertical resolution (20 layers). In Hirota's work no double maximum can be seen in the instability diagrams.

To test further the significance of the secondary instability maximum a non-geostrophic model was derived. The model, described in appendix A, has no vertical variation of the static stability and the vertical wind shear. The perturbations are independent of the y-coordinate. The growth rates were computed and compared to a balanced version of the model. In Fig. 11 is shown a case where the static stability is 2.0 MTS-units, the vertical wind shear 3 m sec^{-1} per 100 mb and $N = 10$.

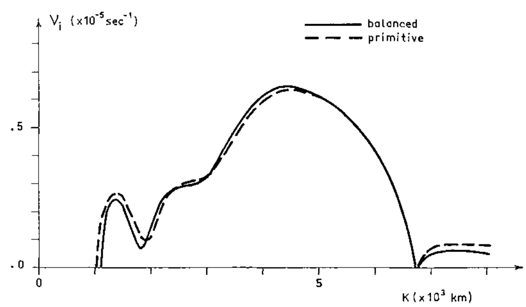

Fig. 11. Growth rates of unstable waves as a function of wavelength K for a primitive and a balanced model. $N = 10$, $s = 2.0$ and the vertical wind shear $\Lambda = 3$ m sec^{-1} per 100 mb.

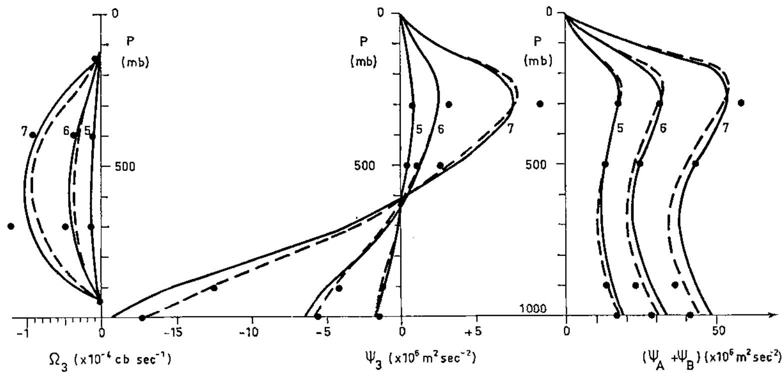

Fig. 12. Amplitudes after 5, 6 and 7 days integration of the induced zonal fields Ω_3 and ψ_3 and the first order perturbation $(\psi_A + \psi_B)$. Dashed lines indicate $N = 9$, full lines $N = 5$ and dots indicate $N = 3$. The wavelengths of the perturbation are $K = 4\ 000$ km and $L = 10\ 000$ km.

The result shows that the secondary instability maximum for short wavelengths is present in both primitive and balanced linearized models of the atmosphere for high vertical resolutions. Figs. 6–9 show that a necessary vertical spacing needed to resolve this type of instability is of the order of 5 levels. At the same time a horizontal resolution of the order of 150 km is essential.

The most interesting results from the computations of the first order solution can be summarized as follows:

1. At least 5 levels in the vertical must be used if a good vertical description of waves within the wavelength interval of normal maximum baroclinicity is desired. The corresponding horizontal gridlength is of the order of 250 km.

2. A low vertical resolution is most serious when the horizontal scale is small.

3. High resolution models have significantly higher instability in the short wave interval 1 000–2 000 km and the first mode of instability is split into two separate maxima, the one with the shortest wavelength is connected with waves concentrated to the lower atmosphere and with a less pronounced back-ward tilt with height.

4. The secondary maximum at short wavelengths is very sensitive to changes in the static stability in the lower part of the atmosphere. The maximum is also present in a linearized primitive model.

5. A necessary spacing needed to resolve this instability is of the order of 5 vertical levels and a horizontal gridlength of 150 km.

8.2. *Induced zonal field*

Numerical time-step integrations were performed up to 7 days. The initial perturbation $(\psi_A + \psi_B)$ was 10^6 m^2 sec^{-1} and the time step 1 hour.

Fig. 12 shows the development of the induced zonal flow and the perturbation $(\psi_A + \psi_B)$ during the integration. The wavelengths are $L = 10\ 000$ km and $K = 4\ 000$ km. Other combinations of wavelengths were also tried, but the characteristic features of the induced zonal fields were not much changed.

The induced zonal streamfunction ψ_3 is negative at the lower levels implying an increased westerly wind in the central part of the zonal flow with eastward components to the north and south.

At higher levels, ψ_3 is positive with a maximum between 200 and 300 mb and the induced zonal wind has an eastward component in the central part of the zonal flow and westerly winds to the north and south.

The effect on the total ψ-field is a northward displacement of the developing low in the the lower atmosphere and a southward displacement of the low centre in the upper atmosphere. This is a well documented feature of middle latitude disturbances. The properties of the induced mean zonal field and its effect on the perturbation have been discussed by Phillips (1954) and Saltzman & Tang (1972).

The induced zonal vertical velocity Ω_3 is also shown in Fig. 12. The circulation is of Ferrel type with rising air north of the maximum zonal flow and sinking air to the south. The maximum vertical velocity is achieved approximately at the level where ψ_3 changes sign, i.e. around 600 mb.

Three different vertical resolutions, $N=3$, 5 and 9, are al: o compared in the figure. In accordance with Fig. 8 the growth rates of the first order perturbation are not exactly equal for the three resolutions and one must expect different induced zonal fields as well. The differences are, however, small and consistent with the different amplitudes of the perurbation. We may therefore draw the conclusion that the induced zonal field can be resolved by a model with a relatively low resolution.

The effect of the induced zonal field back on the first order perturbation is shown in the Figs. 13 and 14. It is seen that the amplitude of $(\psi_A+\psi_B)$ is damped, but the vertical velocity is increased. The induced zonal field also increases the tilting of the perturbation.

8.3. *Second order solution*

A number of integrations up to 7 days were performed with the complete set of orthogonal functions. The dominating part of the second order field was found to be the zonal component ψ_2. The values of ψ_2 were positive, corresponding to a negative contribution in the central part of the zonal flow, i.e. a weakening of the highs and a deepening of the lows.

For the sake of simplicity we introduce the following notations

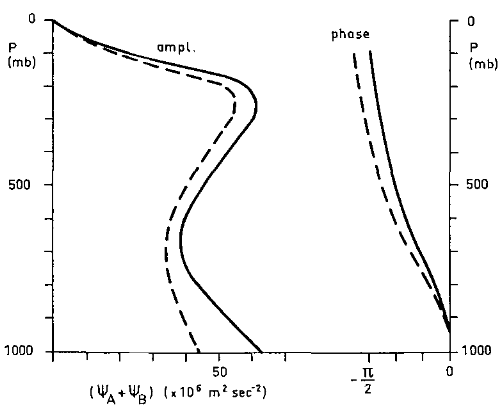

Fig. 13. Amplitude and phase angle of the first order perturbation $(\psi_A+\psi_B)$ after 7 days. Full lines indicate no interaction with the induced zonal field and dashed lines indicate a complete interaction with the induced zonal field $N=9$, $L=10\ 000$ and $K=4\ 000$ km.

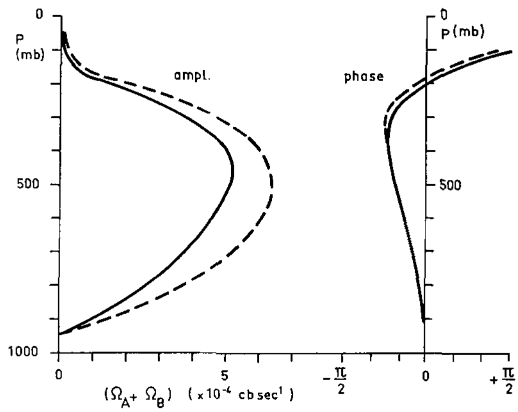

Fig. 14. The same as in Fig. 13 but for $(\Omega_A+\Omega_B)$.

$$\psi^{(1)}=\psi_A+\psi_B$$

$$\psi^{(2)}=\psi_a+\psi_b+\psi_c+\psi_d+\psi_e+\psi_f$$

The Figs. 15 and 16 illustrate some horizontal fields after 7 days integration, Fig. 15 at the 500 mb level and Fig. 16 at 1 000 mb. In Figs. 15*a* and 16*a* is shown the second order perturbation $\psi^{(2)}$ together with the first order and induced zonal fields $(\psi^{(1)}+\psi_1+\psi_3)$. The second order perturbed field has its largest amplitude at the lowest level where the negative extremes coincide with the cyclonic and anticyclonic centres. The positive extremes are weaker. The contribution from the second order terms in the vorticity and thermodynamic equations is thus a deepening of the cyclones and a weakening of the anticyclones near the surface of the earth.

At 500 mb the amplitude of $\psi^{(2)}$ is somewhat smaller. While the first order wave is tilting westward with height the second order wave has a very weak eastward tilt.

The effect of the second order terms at the 500 mb level is an increased cyclonic circulation in the eastern parts of the troughs and ridges and a weaker anticyclonic contribution in the western parts of the troughs and ridges.

In Figs. 15*b* and 16*b* are shown the total streamfunction fields. Some typical features of developing cyclones in the real atmosphere can be recognized, for example the displacement of the surface low to the northeast of the upper low, the southward drifting of the surface anticyclone and the splitting of the westerly 500 mb current in the ridges.

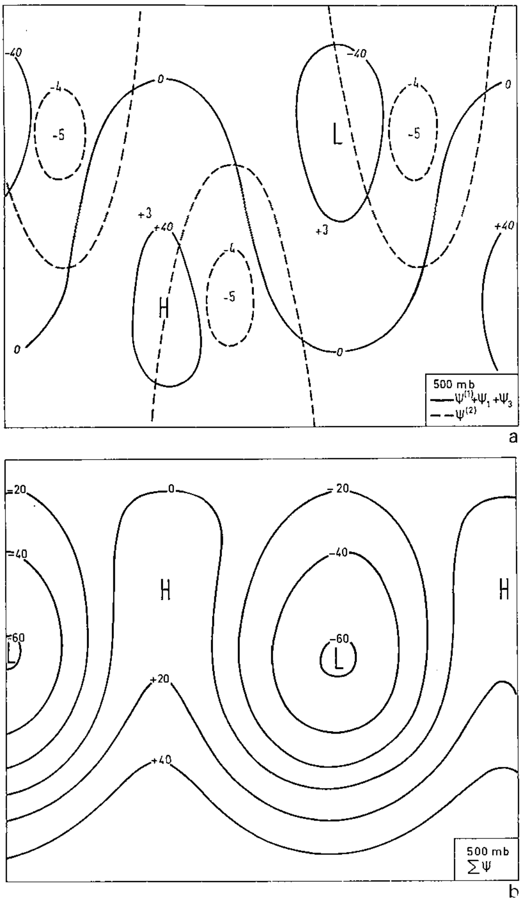

Fig. 15. Streamfunction fields after 7 days at 500 mb level. $N = 9$ and the wavelengths are $K = 4\ 000$ km and $L = 10\ 000$ km. The unit is $10^6\ m^2\ sec^{-1}$. (*a*) Second order perturbation $\psi^{(2)}$ (dashed lines), and first order plus induced zonal fields $\psi^{(1)} + \psi_1 + \psi_3$ (full lines). (*b*) The complete solution $\Sigma\psi$.

The streamfunction fields corresponding to those in Figs. 15 and 16 but for the resolution $N = 3$ showed very small differences.

The integration was repeated with the only difference that the wavelength in the x-direction was 2 000 km. We could recognize the characteristics of a short unstable wave found in the linear theory, i.e. a high amplitude in the lower part and a small amplitude in the upper part of the atmosphere and a small westward tilting with height. The zonal component of the second order solution, ψ_2, was dominating both at 500 and 1 000 mb. The anticyclone centres were very effectively surpressed.

The total streamfunction field at 1 000 mb after 7 days is found in Fig. 17.

The relative importance of each of the four second order terms in the vorticity equation (term I–IV in section 2) was studied by including only one of them at a time and repeating the integrations. The wavelengths were $L = 10\ 000$ km and $K = 4\ 000$ km and $N = 9$. The maximum amplitude of the second order perturbation $\psi^{(2)}$ corresponding to the different terms is shown for the levels 500 and 1 000 mb in Fig. 18. The second order terms represent about 5–10% of the first order perturbation.

Term IV, i.e. the effect of the divergent wind on the advection of absolute vorticity, has a small influence on the solution at both levels. The twisting term, term III, has a larger effect, but the dominating terms are term I,

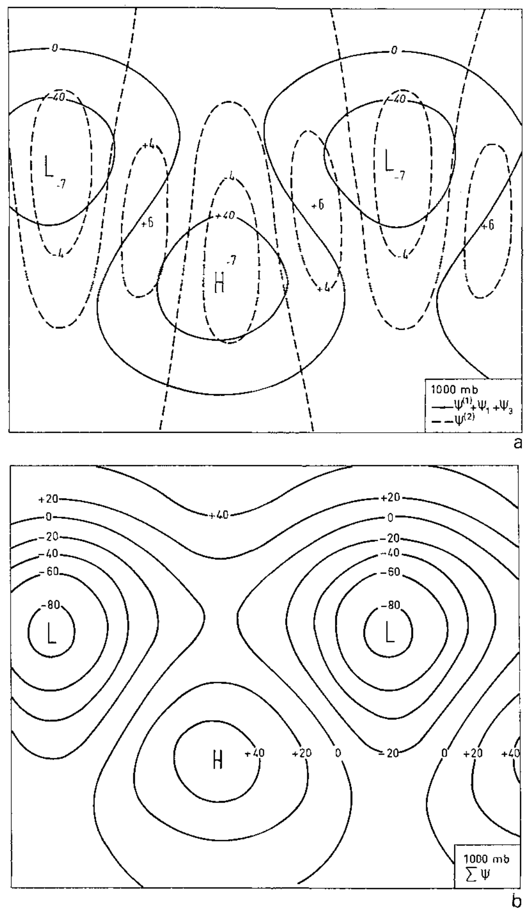

Fig. 16. Same as Fig. 15 but for the 1 000 mb level.

describing the vorticity-divergence effect, and term II, the vertical advection of vorticity. Term I has the largest influence at lower levels and term II at 500 mb.

Compared to the complete second order perturbation (see Figs. 15*a* end 16*a*) the distribution of positive and negative areas is similar for terms I and II, whereas terms III and IV have an opposite distribution.

One property of the complete vorticity equation is that the sum of terms II and III is zero if integrated over a closed surface. In some prediction models it has been assumed that the two terms approximately balance each other locally and that they both can be neglected in the vorticity equation. In this study the two terms do not possess a local balance and the sum of the contribution from the two terms is of the same order as from the individual terms. This indicates the importance of keeping all the smaller terms in the vorticity equation.

The magnitude of the contribution from the term $-\nabla\chi\cdot\nabla(\partial\psi/\partial p)$ in the thermodynamic equation (not shown in Fig. 18) is of the order 3 units at 1 000 mb and 1 unit at 500 mb. The distribution patterns was somewhat different from the other small terms, but the effect was mainly the same as for the sum of all terms, namely a deepening of the cyclones and a weakening of the anticyclones and some increased cyclonic circulation in the eastern parts of the upper troughs and ridges.

The results of the investigation of the second order solution can be summarized as follows:

1. The second order terms in the vorticity and thermodynamic equations add to the solution features characteristic for the real atmosphere.

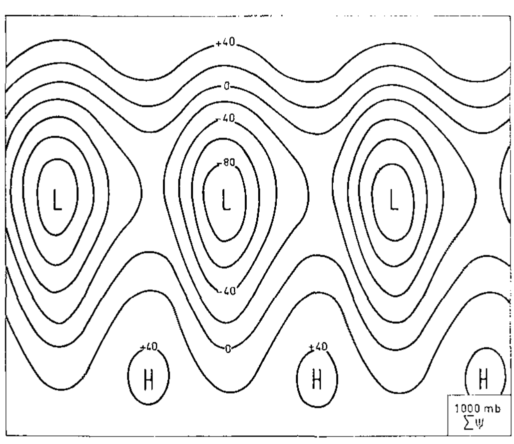

Fig. 17. Same as Fig. 15*b* but for $K = 2\ 000$ km.

2. The contribution is mainly a deepening of the cyclones and a weakening of the anticyclones and an increased cyclonic circulation in the eastern parts of the upper troughs and ridges.

3. The second order terms represent about 5–10% of the first order perturbation energy. *All terms are important.*

4. The effect of the vertical resolution is small.

Acknowledgements

The writer wishes to thank Prof. Bert Bolin for reading the manuscript critically and giving valuable advice and Mrs Kerstin Fabiansen, for typing the manuscript.

Appendix A

A model for non-geostrophic baroclinic instability

The linearized form of the vorticity equation, the divergence equation and the thermodynamic can be written as

$$\begin{cases} \psi_{txx} + U\psi_{xxx} + \beta\psi_x + f_0\chi_{xx} = 0 \\ \chi_{txx} + U\chi_{xxx} + U_p\omega_x + \Phi_{xx} - f_0\psi_{xx} + \beta\chi_x = 0 \\ \theta_t + U\theta_x + \bar{\theta}_y\psi_x + \bar{\theta}_p\omega = 0 \end{cases} \tag{A 1}$$

where ψ, χ, θ, ω and Φ are perturbed streamfunction, velocity potential, potential temperature, vertical velocity and geopotential, all independent of y. The basic zonal flow, U, on which the perturbations are superimposed, is a function of pressure only. We further assume that

$$U = -\bar{\psi}_y \tag{A 2}$$

where $\bar{\psi} = \bar{\psi}(y)$ is the streamfunction in the basic state. The corresponding geopotential field can be solved from the divergence equation

$$\beta U + \bar{\Phi}_{yy} = 0 \tag{A 3}$$

Two of the variables in the system (A 1) can be eliminated by making use of the continuity equation and the hydrostatic relation. These equations can be written as

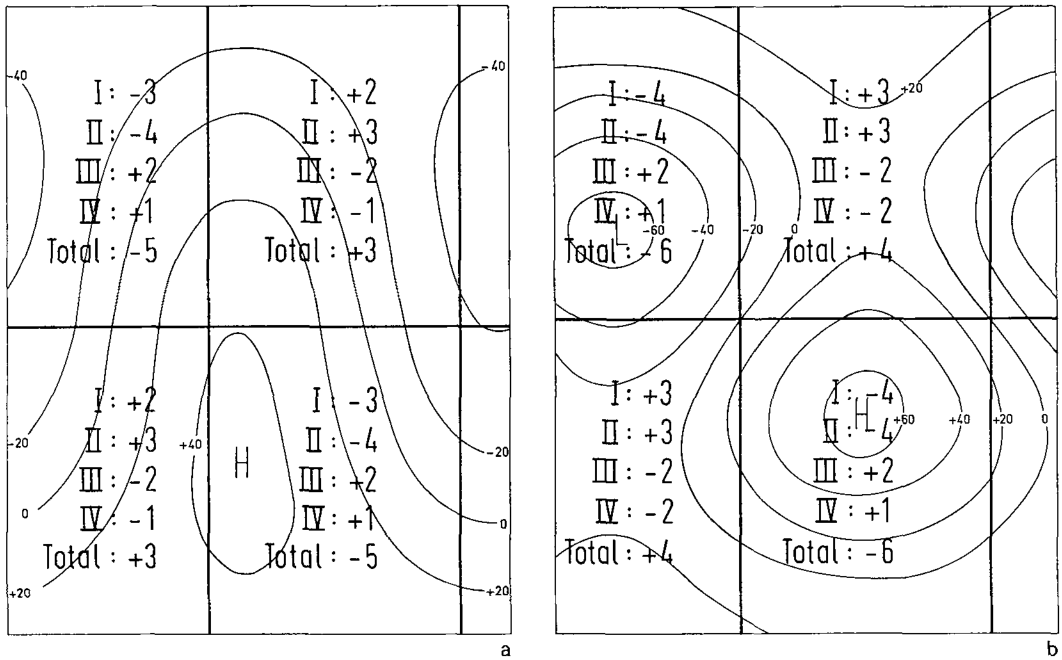

Fig. 18. Schematic presentation of the contributions, $\psi^{(2)}$, from the terms I–IV in the vorticity equation. Approximative extreme values in the four rectangular areas are given for each term. The background fields are $\psi^{(1)}+\psi_1+\psi_3$ at (*a*) 500 mb, (*b*) 1 000 mb. The unit is 10^6 m^2 sec^{-1}.

$$\begin{cases} \chi_{xx}+\omega_p=0 \\ \Phi_p=-Rp_0^{-\varkappa}p^{\varkappa-1}\theta \end{cases} \tag{A 4}$$

where $\varkappa = R/c_p$. The hydrostatic equation applied to the basic state gives a relation between the potential temperature and the geopotential of the basic flow.

$$\bar{\Phi}_p = -Rp_0^{-\varkappa}p^{\varkappa-1}\bar{\theta} \tag{A 5}$$

By eliminating θ and making use of (A 4) and (A 5) we can write the thermodynamic equation in the following form

$$\Phi_{tp}+U\Phi_{xp}-f_0U_p\psi_x+s\omega=0 \tag{A 6}$$

where $s=-\overline{\alpha\cdot\theta^{-1}\cdot\theta_p}$ is the static stability of the mean flow. We now apply perturbations of the form

$$\alpha(x,p,t)=\alpha^*(p)\cdot e^{ik(x-ct)}$$

After the introduction of these wave solutions in the equations (A 1), (A 4) and (A 6) we can eliminate θ^* and χ^* from the resulting system and we obtain the following three equations

$$\begin{cases} c\psi=\left(U-\dfrac{\beta}{k^2}\right)\psi-\dfrac{f_0}{k^3}w_p \\ c\Phi_p=U\Phi_p-f_0U_p\psi-\dfrac{s}{k}w \\ cw_p=\left(U-\dfrac{\beta}{k^2}\right)w_p-U_pw-f_0k\psi+k\Phi \end{cases} \tag{A 7}$$

where w is the imaginary variable $w=i\omega^*$. In (A 7) all star indices (*) are dropped.

We assume a static stability s and a vertical wind shear $U_p=-\Lambda$ independent of pressure and divide the atmosphere into N layers. The boundary conditions are $w=0$ at $p=0$ and $p=1\,000$ mb.

The vorticity and divergence equations are applied to the level j and the thermodynamic equation to the level $j+1/2$

$$\begin{cases} c\psi_j = \left(U_j - \dfrac{\beta}{k^2}\right)\psi_j - \dfrac{f_0}{k^3\Delta p}(w_{j+1/2} - w_{j-1/2}); \\ \qquad\qquad (j = 1, 2, \ldots N) \\ c(\Phi_{j+1} - \Phi_j) = U_{j+1/2}(\Phi_{j+1} - \Phi_j) \\ \qquad + f_0 \Lambda \Delta p \tfrac{1}{2}(\psi_{j+1} + \psi_j) \\ \qquad - \dfrac{s\Delta p}{k} w_{j+1/2}; \quad (j = 1, 2, \ldots, N-1) \\ c(w_{j+1/2} - w_{j-1/2}) = \left(U_j - \dfrac{\beta}{k^2}\right)(w_{j+1/2} - w_{j-1/2}) \\ \qquad + \Lambda \Delta p \tfrac{1}{2}(w_{j+1/2} + w_{j-1/2}) - f_0 k \Delta p \psi_j \\ \qquad + k \Delta p \Phi_j; \quad (j = 1, 2, \ldots, N) \end{cases} \tag{A 8}$$

The system (A 8) can be written in matrix form and the complex phase velocities can be solved as eigenvalues to a matrix of the dimension $3N - 2$. The numerical method used was the same as described in section 6. The solution results in $2N - 2$ combined gravity-inertial waves and N meteorological waves.

The corresponding quasi-geostrophic model was derived by using the simple relation

$$f_0 \psi = \Phi$$

in place of the third equation in (A 7) and eliminating Φ and w from the system.

Appendix B

Time integration

When the induced zonal and the second order flow are included, the system consists of non-linear ordinary differential equations. By replacing the time derivatives by finite differences over a small time step Δt it is possible to solve the system numerically as an initial value problem.

As the initial state, a perturbation $(\psi_A + \psi_B)$ of small amplitude on the stationary zonal flow, ψ_1, is used.

A double step method proposed by Lorenz (1963*a*) is applied. To illustrate the technique we write the system (3) in a simplified formal way as

$$\begin{cases} \dfrac{d\psi_i}{dt} = G \\ \qquad\qquad i = A, B, 3 \\ \Omega_i = H + \dfrac{d\psi_i}{dt} \end{cases} \tag{B 1}$$

where G represents the right hand side of (3a) with $W_i = 0$ and H is the first expression on the right hand side of (3b). G and H contain the variables ψ_1, ψ_A, ψ_B and ψ_3 and non-linear combinations between these variables. The system (B 1) can be solved as a closed system.

For the second order solution the system can be written as

$$\frac{d\psi_j}{dt} = G + V \quad j = a, b, c, d, e, f, 2$$

G now only contains ψ_a, ψ_b ... ψ_f and ψ_2 (all interactions c_{ijk} are zero) and V contains interactions between Ω_i and ψ_i $(i = 1, A, B, 3)$. The V-terms can be evaluated from the solution of system (B 1).

If all variables are known at time t the values at the time $t + \Delta t$ are computed by first making two consecutive forward time steps and then using the mean values between the resulting values and the values at time t.

$$\begin{cases} \psi_i^* = \psi_i^t + G^t \cdot \Delta t \\ \psi_i^{**} = \psi_i^* + G^* \cdot \Delta t \\ \psi_i^{t+\Delta t} = \tfrac{1}{2}(\psi_i^{**} + \psi_i^t) \qquad\qquad (i = A, B, 3) \\ \Omega_i^t = H^t + \dfrac{1}{\Delta t}(\psi_i^* - \psi_i^t) \\ \Omega_i^* = H^* + \dfrac{1}{\Delta t}(\psi_i^{**} - \psi_i^*) \end{cases}$$

$$\begin{cases} \psi_j^* = \psi_j^t + G^t \cdot \Delta t + V^t \cdot \Delta t \\ \psi_j^{**} = \psi^* + G^* \cdot \Delta t + V^* \cdot \Delta t \qquad (j = a, b, c, d, e, f, 2) \\ \psi_j^{t+\Delta t} = \tfrac{1}{2}(\psi_j^{**} + \psi_j^t) \end{cases}$$

The computations must start from the first equation and then continue downwards. For example, V^* is computed by making use of Ω_i^* and ψ_j^* previously evaluated during the same time step calculation.

To get a good accuracy in the computations the time step Δt has to be chosen as a fraction of the shortest period in the solution, i.e.

$$\Delta t \ll \frac{1}{\nu}$$

REFERENCES

Bretherton, F. P. 1966. Critical layer instability in baroclinic flows. *Quart. J. R. Met. Soc. 92,* 325–334.

Brown, J. A., Jr. 1969. A numerical investigation of hydrodynamic instability and energy conversions in the quasi-geostrophic atmosphere. Part I. *J. Atmos. Sci. 26,* 352–365.

Bryan, K. 1959. A numerical investigation of certain features of the general circulation. *Tellus 11,* 163–174.

Charney, J. G. 1947. The dynamics of long waves in a baroclinic westerly current. *J. Met. 4,* 135–162.

Eady, E. T. 1949. Long waves and cyclone waves. *Tellus 1,* 33–52.

Green, J. S. A. 1960. A problem in baroclinic stability. *Quart. J. R. Met. Soc. 86,* 237–251.

Hinkelmann, K. 1959. Ein numerisches Experiment mit den primitiven Gleichungen. In The Atmosphere and the Sea in Motion, pp. 486–500. Rockefeller Press, New York.

Hirota, I. 1968. On the dynamics of long and ultralong waves in a baroclinic zonal current. *J. Met. Soc. Japan 46,* 234–249.

Huss, A. & Mintz, Y. 1962. Growth of a baroclinic wave and evolution of the mean zonal and mean meridional circulations. *Proc. Intern. Symp. Numerical Weather Prediction, Tokyo, 1960, Met. Soc. Japan,* pp. 539–552.

Kuo, H. L. 1952. Three-dimensional disturbances in a baroclinic zonal current. *J. Met. 9,* 260–278.

Kuo, H. L. 1953. The stability properties and structure of disturbances in a baroclinic atmosphere. *J. Met. 10, 235*–243.

Lorenz, E. N. 1960*a*. Maximum simplification of the dynamic equations. *Tellus 12,* 243–254.

Lorenz, E. N. 1960*b*. Energy and numerical weather prediction. *Tellus 12,* 364–373.

Lorenz, E. N. 1963*a*. Deterministic non-periodic flow. *J. Atmos. Sci. 20,* 130–141.

Lorenz, E. N. 1963*b*. The mechanics of vacillation. *J. Atm. Sci. 20,* 448–464.

Palmén, E. & Newton, C. W. 1969. *Atmospheric circulation systems,* pp. 20–22. Academic Press, New York.

Pedersen, K. 1971. Balanced systems of equations for the atmospheric motion. *Geof. Publ. 28,* No. 2.

Phillips, N. 1954. Energy transformations and meridional circulations associated with simple baroclinic waves in a two-level quasi-geostrophic model. *Tellus 6,* 273–286.

Phillips, N. A. 1956. The general circulation of the atmosphere: a numerical experiment. *Quart. J. R. Met. Soc. 82,* 123–164.

Saltzman, B. & Teweles, S. 1964. Further statistics on the exchange of kinetic energy between harmonic components of the atmospheric flow. *Tellus 16,* 432–435.

Saltzman, B. & Tang, C-M. 1972. Analytical study of the evolution of an amplifying baroclinic wave. *J. Atmos. Sci. 29,* 427–444.

Simons, T. J. 1972. On the theory of atmospheric development. *Mon. Wea. Rev. 100,* 145–152.

Wiin-Nielsen, A. 1962. On transformation of kinetic energy between the vertical shear flow and the vertical mean flow in the atmosphere. *Monthly Weather Review 90,* 311–323.

Wiin-Nielsen, A. 1965. Some new observational studies of energy and energy transformations on the atmosphere. *WMO, Technical Note No. 66,* pp. 177–202.

СПЕКТРАЛЬНАЯ МОДЕЛЬ ДЛЯ ИССЛЕДОВАНИЯ УСИЛИВАЮЩИХСЯ БАРОКЛИННЫХ ВОЛН

Для исследования эффекта вертикального разрешения на поведение бароклинных волн исследуется спектральная квазигеострофическая модель с аппроксимацией вертикальных производных конечными разностями. Исследуется также эффект малых членов в полных уравнениях вихря и термодинамики. Эти члены разбираются отдельно и модифицируют растущую волну первого порядка и индуцируемые зональное поле. Бароклинная неустойчивость по отношению к возмущениям первого порядка вычисляется для различных волновых номеров в x- и y-направлениях. Численные эксперименты показывают, что низкое вертикальное разрешение приводит к наибольшим последствиям, когда горизонтальный масштаб мал. Модели с высоким разрешением приводят к большей неустойчивости для коротковолнового интервала 1 000–2 000 *км;* неустойчивость распадается на два отдельных максимума. Вторичный максимум на самых коротких волнах очень чувствителен к изменениям статической устойчивости и присутствует также в линеаризованной примитивной модели. Пространственный шаг, необходимый для разрешения этой неустойчивости составляет около 5 уровней по вертикали и 150 *км* по горизонтали. Найдено, что эффект вертикального разрешения на индуцируемый зональный поток и поля второго порядка очень мал. Вклад малых членов в полных уравнениях сказывается главным образом в углублении циклонов, ослаблении антициклонов и возрастании циклонической циркуляции в восточных частях ложбин и гребней в верхней тропосфере. Изучается сравнительное значение каждого малого члена и сделан вывод о важности сохранить их все вместе.